Physica B 185 (1993) 528–538
North-Holland

PHYSICA B

Properties of interfaces of diamond

R.J. Nemanich, L. Bergman, K.F. Turner, J. van der Weide and T.P. Humphreys

Department of Physics and Department of Materials Science and Engineering, North Carolina State University, Raleigh, NC, USA

Results related to two different interface aspects involving diamond are described: (1) the initial states of CVD diamond film growth, and (2) the negative electron affinity and formation of metal–diamond interfaces. The surface and interface properties are probed with STM, Raman scattering/photoluminescence and angle-resolved UV photoemission spectroscopy (ARUPS). STM measurements of diamond nuclei on Si after various plasma growth processes show both flat and hillocked structures characteristic of 2-dimensional and 3-dimensional growth modes, respectively. STS measurements show distinct I–V characteristics of the nuclei and the substrate. The presence of optical defects and the diamond quality are studied with micro-Raman/photoluminescence measurements. The results indicate an increased density of impurity-related defects during the initial stages of growth. The interface properties of Ti on natural crystal (1 1 1) and (1 0 0) surfaces are studied with ARUPS using 21.2 eV HeI emission. Prior to deposition the diamond (1 1 1) is chemically cleaned, and a sharp (0.5 eV FWHM) peak is observed at the position of the conduction band minimum, indicating a negative electron affinity surface. After a subsequent argon plasma clean this peak disappears, while the spectrum shows a shift of 0.5 eV towards higher energies. Upon sub-monolayer titanium deposition on (1 1 1) diamond, the negative electron affinity peak reappears. Further titanium depositions causes this titanium-induced negative electron affinity peak to be attenuated, indicating that the emission originates from the interface. A similar experiment, done on the diamond (1 0 0) surface, however, does not result in a negative electron affinity. By determining the relative positions of the diamond valence band edge and the titanium Fermi level, the Schottky barrier height of titanium on diamond is measured. A model, based on the Schottky barrier height of titanium on diamond, and the work function of titanium, is proposed for the observed titanium-induced negative electron affinity.

1. Introduction

Continuing advances in the CVD growth of doped diamond thin films offer the possibility of diamond semiconductor devices [1]. Because large diamond substrates are, at this time, prohibitively expensive, most potential electronic applications have focused on heteroepitaxial structures. The nucleation of diamond on non-diamond substrates has, however, proved difficult. Because of the potential for electronic applications, much effort has been focused on the nucleation and growth of diamond on Si. While small regions of heteroepitaxial growth have recently been reported on SiC and BN substrates [2,3] only polycrystalline growth has been achieved on Si and other commonly used substrates. In fact, without special processing of the substrate, the initial nucleation rate is so low, that no diamond growth is achieved within an exposure to the growth conditions for over 60 min. In this study, the initial growth nucleation and growth modes of diamond on Si are studied by STM and Raman photoluminescence measurements.

To achieve diamond devices, metal contacts and Schottky barriers will be critical. One of the most important advances with regards to device applications is the growth of p-type diamond with boron incorporation. This is achieved either by implantation or by incorporation during the growth. Device structures have been demonstrated with the p-type material, and it is apparent that understanding contacts and Schottky

Correspondence to: R.J. Nemanich, Department of Physics and Department of Materials Science and Engineering, North Carolina State University, Raleigh, NC 27695-8202, USA.

barrier properties will be critical. Because of the large band gap, diamond has the potential of high temperature operation, thus it is critical to obtain contacts and Schottky barrier structures that are both chemically and electrically stable at high-temperature operation.

A particularly interesting property of diamond is that under some surface preparation conditions, a negative electron affinity can be achieved. The term negative electron affinity means that the conduction band of the semiconductor at or near the surface is above the vacuum level (i.e. the zero kinetic energy of an electron in free space). In this condition electrons in the conduction band will not be bound in the sample and electron emission can occur. In this study we demonstrate that the electron affinity is dependent on the sample surface preparation. Both surface termination and overlayer coverage can substantially affect the electron affinity.

2. Experimental

The diamond films were prepared by microwave plasma CVD on 1 inch diameter n-type Si(1 1 1) or Si(1 0 0) substrates. The substrates were polished with 0.25 μm diamond powder, followed by an ultrasonic clean in TCE, acetone, methanol, a rinse with de-ionized water and then a drying with nitrogen. A 30 minute hydrogen plasma etch was performed before growth. The growth occurred at a pressure of 25 Torr, a methane to hydrogen ration of 1% with a total flow rate of 1000 sccm and a substrate temperature of ~750°C. No intentional dopant was used in the growth process. SEM micrographs were obtained of the surfaces to show the surface topography on a large scale and to provide an estimate of the nucleation density and the evolution of growth on the surface. Raman spectroscopy and photoluminescence analysis were also performed. The subsequent growth was observed by stopping the growth process after 1.5, 3, 5, 7, 10, 17 and 40 hours of deposition.

The STM analysis of the diamond was done over a wide range of parameters. All of the analysis was performed using an Park Scientific Instruments SU-200 scanning tunneling microscope operated in the ambient atmosphere. The surfaces were scanned over several scan ranges (20 Å–5 μm), tunneling currents (0.5 nA–4.0 nA) and at both positive- and negative-bias voltages. With the STM used, a positive-bias voltage corresponds to a voltage applied to the tip that is positive relative to the sample.

Current–voltage measurements were also performed using the STM, in a process that is called tunneling spectroscopy. In these measurements, the bias voltage is ramped from positive to negative volumes, and the current monitored. All current–voltage measurements presented are averaged over many voltage cycles and were representative of the I–V characteristics of the entire surface. Measurements also allowed for measurement of the surface density of states, which is proportional to the ratio of the differential conductance to the conductance.

The photoemission data presented in this paper, were obtained from natural single crystal diamond. The diamond substrates used in this study were $3 \times 3 \times 0.5$ mm^3, type IIb wafers, with a (1 1 1) or a (1 0 0) surface orientation. These wafers are p-type semiconducting, with typical resistivities ranging from 1.3 kΩ cm to 16 kΩ cm. The substrates were polished with 0.25 μm diamond grit and cleaned in a boiling chromic acid solution before loading. Once in a vacuum the diamond (1 1 1) was further cleaned in a plasma cleaning chamber by exposing it to a remote, RF induced, argon plasma. During the exposure the diamond was heated to 350°C. The diamond (1 0 0) was cleaned by heating it in UHV to about 600°C for 10 min. Titanium was evaporated by resistively heating a titanium filament, and spectra were taken at increasing thicknesses. The thickness of the deposited films was monitored with a crystal rate monitor. The plasma cleaning chamber is connected to the ARUPS chamber through an UHV transfer system. The photoemission was excited with 21.21 eV HeI radiation, and the data presented here was obtained with an angle-resolved ultraviolet photoemission spectroscopy (ARUPS) system, which included a 50 mm radius hemi-

spherical analyzer with an angular resolution of 2°. A bias voltage of ~1 V or less, was applied to the sample during the measurements to overcome the work function of the analyzer. The bias voltage allowed the collection of the low energy electrons, which show the negative-electron-affinity effect.

3. Results and discussion

3.1. Nucleation and initial growth

The results of the investigation of the initial stages of diamond growth can be broken down into different properties: changes in the surface which occur during growth, observation and analysis of the nuclei formed during growth, and the electronic properties of the nuclei and the substrate surface. STM analysis of diamond and diamond-like materials has been described in several recent studies. Previous works using STM by the authors have examined topography of CVD-doped diamond films and undoped nuclei, changes in the growth surface and nuclei during growth, and examination of Ni contacts to single-crystal diamond [4–6]. Tsuno et al. have examined homoepitaxial CVD diamond films grown on the diamond (0 0 1) surface and observed surface reconstructions [7]. Everson and Tamor have investigated the structure of doped nuclei grown on silicon [8]. The only group to report successful STM examination of thick undoped diamond films has come from Busmann et al. [9]. Several other groups have examined amorphic diamond and diamond-like carbon [10–14]. Discussions of the theory and practice of imaging diamond can be found in these references.

The changes in the surface which occur during growth can be examined before the first observation of nucleation. Figure 1 shows the surface structure of one of the samples as viewed by STM. Comparisons of the 30 minute and the 60 minute growth samples showed that the surface of the 60 minute sample appeared to be rougher than the 30 minute sample. Neither sample showed diamond nucleation. The surface, however, showed an increased roughness for the longer growth. This indicates the formation of a surface layer, presumably SiC or disordered carbon.

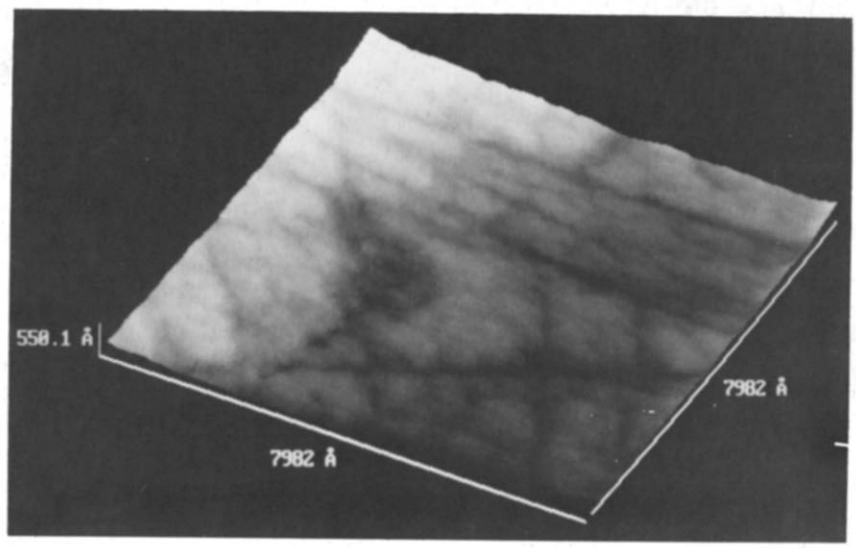

Fig. 1. STM micrograph of the scratched Si surface after a 60 minute exposure to plasma growth conditions. Scratches can be seen on the substrate which have been used to increase the nucleation density. The roughness of this sample provides evidence of plasma-induced surface modification preceding diamond nucleation.

During the initial phase of the growth process examined here, a majority of nuclei exhibit a 3-dimensional structure. A minority of the nuclei do exhibit a more 2-dimensional structure, which indicates a 2-dimensional growth mode. Figure 2 shows both flat and hillocked structures characteristic of 2-dimensional and 3-dimensional growth modes, respectively. The top of the flat nucleus shown is smooth to within ~20 Å and has a 'height' to 'width' ratio of 1:4. The surface

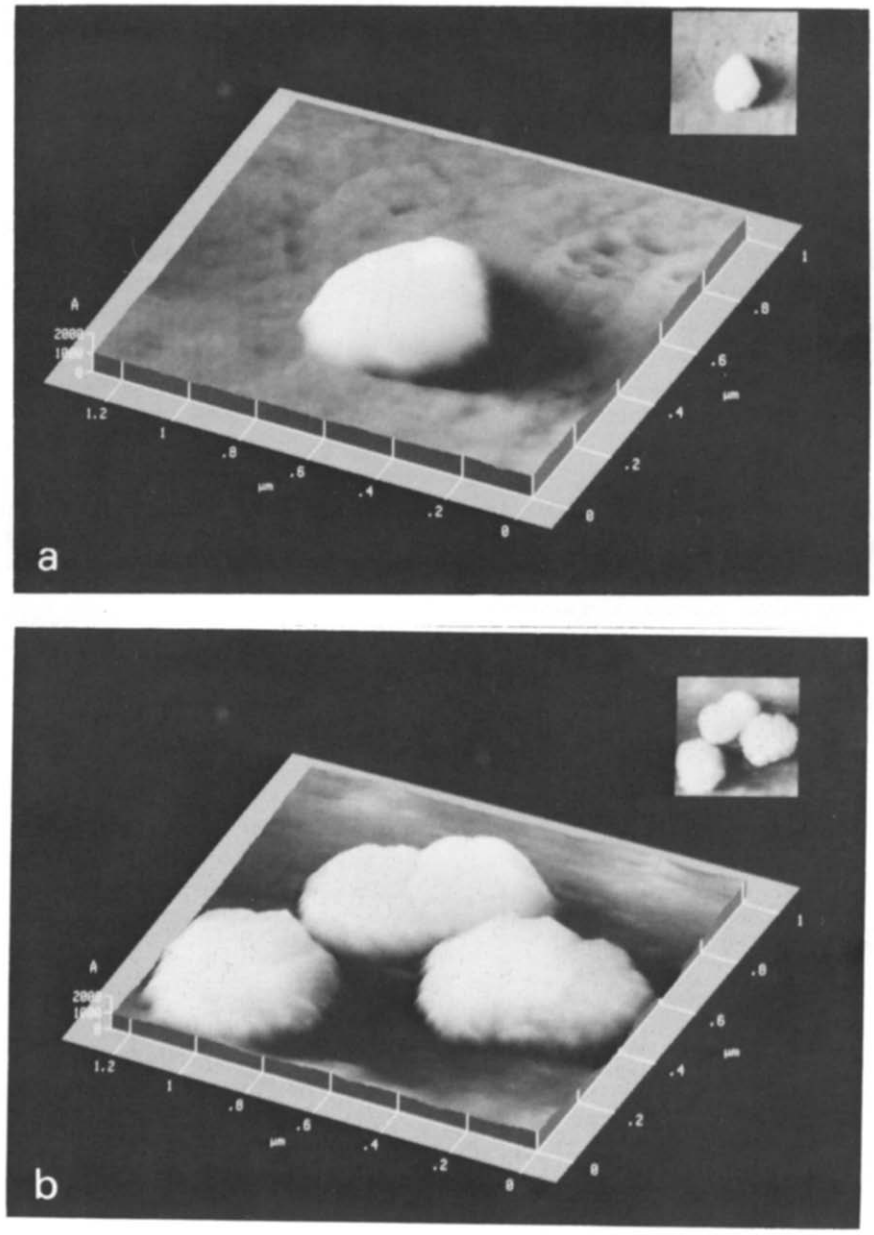

Fig. 2. STM images of diamond nuclei on Si. The upper STM micrograph shows a nucleus of diamond grown on silicon that is exhibiting a flat surface nearly parallel to the substrate. The lower micrograph shows several nuclei that are growing 3-dimensionally. Both types of nuclei were found on the same silicon substate after 1 hour of deposition.

of the nucleus is parallel to the substrate and indicates that the interactions with the substrate contribute to the growth and morphology. This is an important aspect because it is likely that the initial diamond has formed in the scratched regions. We would suggest that it is possible that the initial diamond formation in the scratches is highly disordered, thus allowing the substrate interactions to contribute to determination of the growth morphology. The second image shows several nuclei, one of which appears to be twinned, which have 'height' to 'width' ratios of ~1:2. The fact that both types of nuclei were observed after the same exposure to growth, supports the fact that two distinct modes exist and that the 2-D mode is not merely an early manifestation of a 3-D growth mode. Evidence of this 2-dimensional mode is interesting because it may be an indication that conformal growth is possible and if it could be enhanced, creating planer diamond films with fewer polycrystaline domains might be possible.

Tunneling spectroscopy measurements show distinct I–V characteristics of the nuclei and the substrate. Examples of I–V curves obtained from different points are shown in fig. 3. The ability to distinguish between the types of materials on the surface is an important one. The curve obtained by tunneling to the diamond nucleus is smoothly varying and shows little response at positive bias voltages. The substrate I–V curve shows much more structure including a large change in the current starting at +2.5 V. The 'peaks' in the I–V curve taken over the substrate are indicative of the electronic structure of the carbonic layer that has formed on the substrate during growth. These 'peaks' may be a result of absorbates, bonded to the silicon, which are weakly connected to bulk states.

The ability to carry out tunneling experiments from undoped diamond regions is in itself unique since diamond has such a high electrical resistivity. To probe the defect and impurity properties of the initial stages of growth, micro-photoluminescence measurements were carried out as a function of growth time. In this experiment, the same sample was measured after various growth times. A relatively strong feature was observed in the micro-photoluminescence at an emission energy of 1.68 eV, which is shown in fig. 4. There has been considerable discussion about the origin of this feature. It occurs at an energy near to that of the GR1 peak in single-crystal diamond. This feature has been assigned to a neutral vacancy. Since vacancies are mobile in

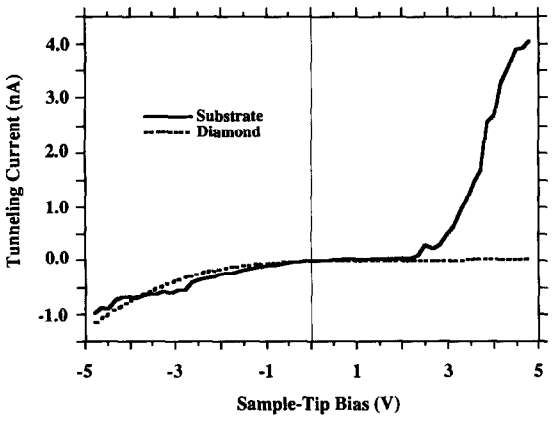

Fig. 3. A comparison of the scanning tunneling spectroscopy current–voltage characteristics of a diamond nucleus and areas of the substrate near the nucleus.

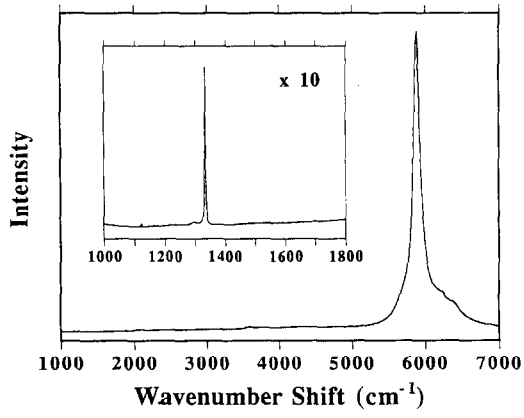

Fig. 4. The Raman/photoluminescence spectrum of CVD diamond after 7 hours of growth. The spectrum was excited with 514.5 nm Ar ion laser light. The spectrum is dominated by the 1.68 eV photoluminescence center for a CVD diamond, and the inset shows an expanded higher-resolution scan over the region of the diamond-sp^2 Raman peaks. At this growth time, the emission from the 1.68 eV PL center showed a maximum relative to the intensity of the diamond Raman.

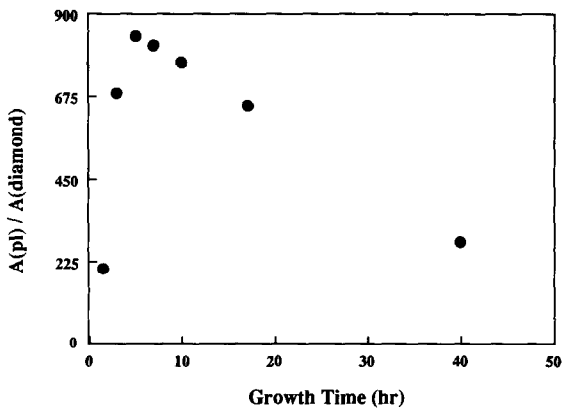

Fig. 5. The integrated intensity of the 1.68 eV PL center relative to the diamond Raman peak as a function of deposition time. A maximum is observed after ~7 hours of growth.

diamond at temperatures ~800°C, it is unlikely that the 1.68 eV feature in the CVD films (growth temperature ~800°C) is due to a vacancy. It has also been suggested that the feature is due to a complex involving Si and/or N [15,16].

The results of the experiment are shown in fig. 5. The relative intensity of the 1.68 eV feature to the Raman diamond feature reaches a maximum after ~7 h and then is reduced with increased growth time. The absolute intensity of the 1.68 eV feature actually increases at least up to a growth time of 15 h (at this time the substrate is nearly completely covered). Thus we can conclude that there is initially a higher rate of impurity incorporation in the film. From the data, it can also be concluded that a higher concentration of defect centers exists near the interface between the diamond and the silicon, with a lower concentration found in the bulk. It is now well established that Si is etched in the presence of atomic H, with SiH_4 being released. We suggest that the observed photoluminescence trend is due to the incorporation of Si which has been etched from the substrate. The rate of incorporation decreases when the Si substrate is covered by diamond after subsequent growth.

3.2. Schottky barrier height measurement

Diamond–metal interfaces and their properties as electrical contacts have received recent attention, and both ohmic and rectifying contacts to both natural diamond and CVD-grown diamond have been reported [6,17–21]. To fully understand the rectifying contact it is necessary to determine the Schottky barrier characteristics. Current–voltage measurements of the rectifying contacts typically show a high ideality factor and cannot be used for an accurate Schottky barrier determination [22]. Photoemission, however, has been successfully used to measure the Schottky barrier height of Al and Au on diamond [23].

Previous current–voltage measurements have demonstrated that titanium, deposited at room temperatures, forms a rectifying contact to p-type diamond. Upon annealing to >400°C the current–voltage characteristics become ohmic [21]. It has been suggested that this transformation is due to the formation of a titanium carbide [17]. In a previous study we have shown that titanium carbide formation does indeed occur in the same temperature range in which titanium contacts are found to change from rectifying to ohmic [24]. In this paper we report a UV photoemission study of thin titanium layers deposited on a diamond (1 1 1) surface. From the measurements, the Schottky barrier height of titanium on p-type diamond (1 1 1) is determined.

The Schottky barrier height of a metal on a p-type semiconductor is defined as the difference between the valence band edge of the semiconductor and the Fermi level of the metal at the interface. The determination of the Schottky barrier height from UV photoemission, relies on the fact that features of both the metal and the underlying semiconductor are visible in one spectrum. Experiments are therefore limited to thin metal films with a thickness on the order of the mean free path of the electrons (~5 Å). Even at metal coverages less than the mean free path, it is not always possible to determine the position of the valence band edge accurately from the spectra, since emission from the metal d-band obscures the relatively weak semiconductor valence band emission. In those cases, a more accurate determination can be made, by relating the valence band edge to a feature in the diamond spectra that does remain visible at high-

er metal coverages. In this analysis it is assumed that shifts in the diamond features are uniform so that relative positions are maintained. In the experiments on the (1 1 1) surface, the valence band edge was determined from the spectrum of the argon-plasma-cleaned diamond and related to a stronger emission feature at lower energies, labeled B, in fig. 6. Although this diamond feature was attenuated upon metal coverage, it remained much more visible than the valence band edge. In order to determine the valence band edge from the position of peak B, their relative positions should not change upon titanium deposition. Since the relative positions of feature B and the valence band edge did not change after the first metal depositions in which both were visible, we do not expect this to occur at the higher metal thicknesses.

The location of the valence band edge was determined by extrapolating the spectrum to zero, as illustrated in fig. 7. The valence band edge was found to be 8.2 eV above feature B. After the first titanium deposition the diamond spectrum shifted 0.5 eV towards lower energies, indicating a change in the pinning position of the Fermi level in the gap. No Fermi level emission due to the titanium could be discerned, however,

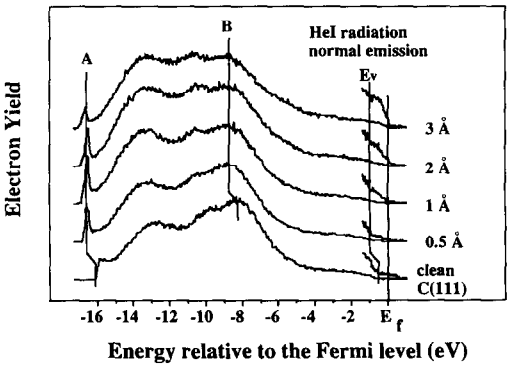

Fig. 6. ARUPS spectra of titanium on diamond (1 1 1) for increasing titanium thicknesses. After the first deposition the spectrum shifts 0.5 eV toward lower energies and a sharp peak (A), indicative of a negative electron affinity, develops at the low-energy cutoff. For increasing titanium thicknesses a Fermi level edge (E_f) develops, while at the same time the position of the valence band edge (E_v) becomes harder to locate. The Schottky barrier height is the energy difference between E_v and E_f.

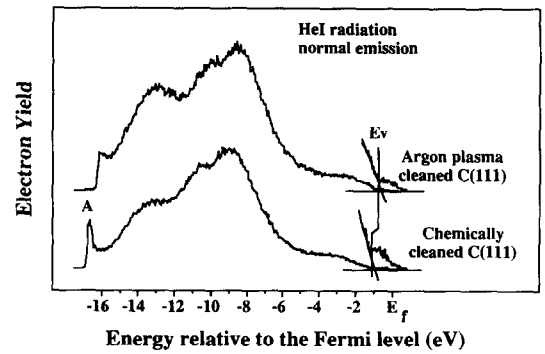

Fig. 7. ARUPS spectra of diamond (1 1 1) before and after argon plasma cleaning. The spectrum shifts by 0.5 eV towards higher energies while the negative electron affinity peak (A) is significantly reduced after the argon plasma cleaning. The latter effect is attributed to the removal of hydrogen from the surface. The valence band edge is determined by linearly extrapolating the onset of emission down to zero.

at this coverage. Upon further titanium deposition, emission from the d-bands of titanium became pronounced, and the Fermi level could be clearly discerned. The position of the valence band edge, however, became more difficult to locate. Based on the position of feature B, no further shifts in the diamond spectrum were observed. This indicates that the Fermi level was pinned, and the Schottky barrier height established, after the first titanium deposition. The Fermi level was found to be 9.2 eV above feature B. Since the valence band edge was 8.2 eV above B this results in a Schottky barrier height for titanium on p-type diamond (1 1 1) of 1.0 ± 0.2 eV.

Similar measurements were performed for titanium on the diamond (1 0 0) surface, as shown in fig. 8. The position of the valence band edge, relative to peak B, was determined again from the clean diamond (1 0 0) surface, and was found to be 8.0 eV, in agreement with the value found from the (1 1 1) surface. No shifts were observed before cleaning, and no significant shifts occurred upon titanium deposition. The position of the Fermi level was determined, and found to be 9.4 eV above feature B. The Schottky barrier height of titanium on the diamond (1 0 0) surface was therefore found to be 1.5 ± 0.2 eV. Reported values for the Schottky barrier

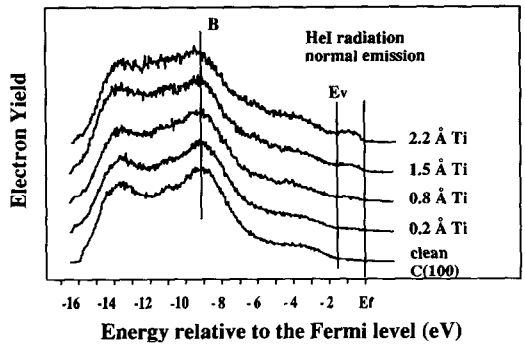

Fig. 8. ARUPS spectra of titanium on diamond (1 0 0) for increasing titanium thicknesses. The position of E_v relative to peak B is determined from the clean surface and is found to be 8.0 eV. The Fermi level is found from the metal-covered diamond (1 0 0) and lies 9.4 eV above peak B, resulting in a Schottky barrier height of 1.5 ± 0.2 eV.

height of titanium on CVD-grown diamond films range from $0.9(+0.5/-0.2)$ eV [24] to 1.3 eV [25].

3.3. Negative electron affinity

The relation between the bands of a semiconductor and the vacuum level can be described by the electron affinity. This quantity which is the energy difference between the conduction band minimum and the vacuum level, is an important parameter in the Schottky–Mott model for Schottky barrier heights. The electron affinity is however dependent on the surface structure of the crystal. A dipole layer on the surface will shift the potential of the material with respect to the vacuum, thus changing the electron affinity. The dipole layer can result from surface structures such as reconstruction or molecular absorption or interface structures such as Schottky barriers or heterojunctions.

Photoemission spectra of negative-electron-affinity surfaces generally show a sharp peak at the low-kinetic-energy end of the spectrum. This peak is attributed to emission of electrons that are quasi-thermalized to the bottom of the conduction band of the semiconductor. For materials with a positive electron affinity, the conduction band minimum is below the vacuum level, and the quasi-thermalized electrons are trapped in the sample. In the experiments described here, the presence of a sharp peak at the onset of the photoemission will be considered as an indication of a negative-electron-affinity surface.

3.3.1. Hydrogen-terminated surfaces

We initiated the study of the negative electron affinity of diamond by verifying the experiment of Pate et al. [26] in which the relation between the negative electron affinity effect and the presence of hydrogen on the surface is established. The H-terminated surfaces were obtained by polishing and etching a diamond (1 1 1) wafer. Followed by a low-temperature anneal (350°C) to desorb contaminants. Photoemission spectra from the diamond before and after thermal desorption of the hydrogen are shown in fig. 9. The negative electron affinity of the surface, which results in the sharp peak at the low-energy end of the spectrum, has clearly been removed from the surface. Since the annealing temperature used to obtain the effect is the same as the reported temperature for the desorption of hydrogen, this suggests that hydrogen on the surface plays a role in the negative electron affinity effect. The spectra of the diamond before and after annealing are followed by spectra from the diamond after exposure to molecular and mono-atomic hydrogen. As is shown in fig. 9, the molecular hydrogen has no effect on the electron affinity of the surface. The mono-atomic hydrogen, however, returned the surface to a negative-electron-affinity state. The fact that exposure to mono-atomic hydrogen causes the surface to exhibit a negative electron affinity confirms that the hydrogen is associated with the negative electron affinity. The difference between the results after exposure to molecular and mono-atomic hydrogen suggest that the hydrogen has to be chemically bonded to the surface. The series is concluded by a spectrum of the diamond after another high temperature anneal, which shows that the cycle is repeatable.

In a second series of experiments, described in fig. 10, the diamond (1 1 1) was exposed to a hydrogen plasma after loading, and the spectrum shows the presence of a negative electron affinity. After a subsequent exposure to an argon

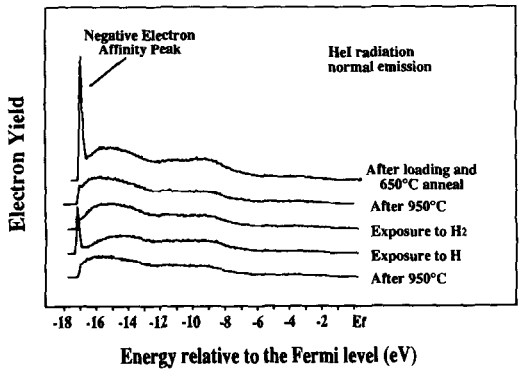

Fig. 9. ARUPS spectra of diamond (1 1 1). The as-loaded spectrum (top) shows the presence of a sharp peak at the lowest energy indicating a negative electron affinity. After a 950°C anneal the peak is gone, indicating the absence of a negative electron affinity. No significant changes occur after exposure to molecular hydrogen for 5 minutes at 10^{-6} Torr. After exposure to mono-atomic hydrogen however the negative electron affinity returns. The bottom spectrum, after another 950°C anneal, shows that the cycle can be repeated.

plasma, however, the sharp peak that is associated with a negative electron affinity, was absent. Since the negative electron affinity is associated with the presence of hydrogen on the surface we conclude that the argon plasma removed the hydrogen from the surface. Exposure to another hydrogen plasma causes the negative electron affinity effect to reappear. This is to be expected in light of the first experiment where exposure to mono-atomic hydrogen also caused the negative electron affinity to reappear.

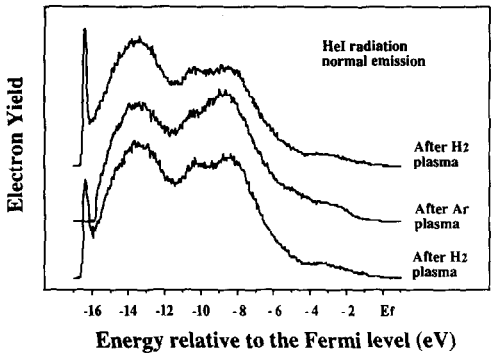

Fig. 10. ARUPS spectra of diamond (1 1 1) after exposure to (from bottom to top) a hydrogen plasma, an argon plasma and a hydrogen plasma. The diamond was heated to approximately 350°C during each exposure. The spectrum after the first hydrogen plasma shows a sharp peak, due to the negative electron affinity of the surface. In the second spectrum, after argon plasma exposure, the peak is absent, indicating a positive or zero electron affinity. In the third spectrum the negative electron affinity is seen to reappear, after exposure to another hydrogen plasma.

3.3.2. *Metal-induced negative electron affinity*

The potential of metals inducing a negative electron affinity were explored. In this case the initial starting surface was a diamond (1 1 1) surface treated with a remotely excited Ar plasma to induce a surface with a slightly positive electron affinity. After the first titanium dose, a sharp peak, similar to the one found on the hydrogen-passivated diamond (1 1 1) surface, develops at the low-energy end of the spectrum. In the same spectrum a 0.5 eV shift towards lower energies is observed. For increasing titanium coverages the peak is attenuated, and no further shifts in the diamond features are observed. We attribute this peak to a titanium-induced negative electron affinity. This would be due to a lowering of the work function by the titanium, as illustrated in fig. 11. Before the titanium deposi-

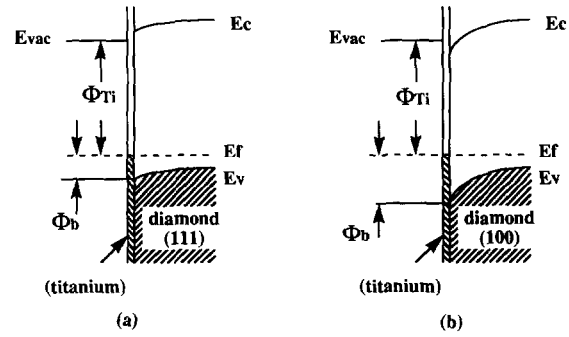

Fig. 11. Model for the titanium-induced negative electron affinity on diamond (1 1 1). In (a) the sum of the work function of the titanium (Φ_{Ti}) and the Schottky barrier height of titanium on the diamond (1 1 1) surface (Φ_{Ti}) is less then the bandgap of the diamond. This lowers the effective work function of the surface such that the conduction band minimum is above the vacuum level, thus resulting in a negative electron affinity. For the diamond (1 0 0) surface (b) however the Schottky barrier height with the titanium is larger than the Schottky barrier height on the diamond (1 1 1) surface, and the sum of the Schottky barrier height and the work function of titanium is more than the bandgap of the diamond, resulting in a positive electron affinity.

tion the Fermi level at the surface is 0.5 eV above the valence band edge. The vacuum level was determined from the low-energy cutoff point of the emission, and is found to be about 5.5 eV above the valence band edge. Using a value of 5.45 eV for the bandgap of diamond we find therefore the vacuum level to be ~0.05 eV above the conduction band edge; electrons that are quasi-thermalized to the bottom of the conduction band are therefore unable to escape the surface. After the first sub-monolayer of titanium is deposited, the Fermi level is pinned at 1.0 eV above the valence band edge, which is the Schottky barrier height described in the previous section. The effective work function of the surface is now determined by the work function of the titanium. Using the value of 4.33 eV for the work function of bulk titanium [27] we find that the vacuum level of the surface is now located 0.2 eV below the conduction band edge and quasi-thermalized electrons can escape, causing the sharp peak in the spectrum. The fact that this peak is due to the interface of the diamond and the titanium, can be deduced from the attenuation of the peak as a function of coverage. Note that in this model the Schottky barrier height plays an important role in determining the position of the vacuum energy level. In fig. 10(b) the titanium–diamond(1 0 0) interface is described. Here the Schottky barrier height is 1.5 eV and the vacuum level lies now above the conduction band edge. Based on this model we do not expect a negative-electron-affinity surface. This is supported by the data, as can be seen in fig. 8. No low-energy peak appears upon titanium coverage. It should be noted, that the model presented here, is the reverse from the Schottky–Mott model. There the Schottky barrier height is determined by aligning the vacuum levels of the metal and the semiconductor.

4. Conclusions

The initial stages of diamond growth show both substrate interactions which lead to non-diamond structures and diamond nuclei which form at scratches on the surface. Even though the initial diamond formation occurs in the scratches, the nuclei growth morphology is related to the substrate. We propose that the initial diamond formation is highly disordered and that as the growth proceeds beyond the scratches, the substrate interactions contribute to the growth morphology. Because of the high resistivity of undoped diamond, tunneling to these structures was not anticipated. Defect structures were observed in the microphotoluminescence measurements. These defects were apparently associated with Si impurities which were due to etching of the exposed substrate.

From the UV photoemission spectroscopy measurements presented here, a Schottky barrier height of 1.0 ± 0.2 eV was found for the titanium–diamond(1 1 1) interface, and 1.5 ± 0.2 eV for the titanium–diamond(1 0 0) interface. It was found that the Schottky barrier heights were established for sub-monolayer titanium coverages. Upon titanium deposition on the diamond (1 1 1) surface, a sharp (0.5 eV FWHM) peak developed at the position of the conduction band edge. This is indicative of a negative-electron-affinity surface. Negative-electron-affinity surfaces are commonly obtained on III–V semiconductors by depositing a thin layer of a low work function material such as cesium or cesium-oxide. This study shows that it is possible to obtain a negative electron affinity on diamond (1 1 1) by depositing a sub-monolayer of a titanium, and suggests the possibility of inducing a negative electron affinity on diamond using other transition metals. A model for the observed negative electron affinity was presented, based on the Schottky barrier height of the diamond–metal interface, and the work function of the metal.

Acknowledgements

We thank B. Stoner and J.T. Glass for providing the initial diamond growth films, K. Das of Kobe Research for his help in establishing the diamond cleaning procedure, T.P. Schneider for the plasma cleaning work, and R. Rudder and

R. Markunas of RTI for helpful discussions. This work is supported in part by the ONR through grants N00014-92-J-1477, N00014-90-J-1604 and N00014-90-J-1707, the NSF through grant DMR 9204285 and the MITI of Japan through the NEDO program.

References

[1] R.J. Nemanich, Ann. Rev. Mater. Sci. 21 (1991) 535.
[2] B.R. Stoner and J.T. Glass, Appl. Phys. Lett. 60 (1992) 698.
[3] S. Koizumi, T. Murakami, T. Inuzuka and K. Suzuki, Appl. Phys. Lett. 57 (1990) 563.
[4] K.F. Turner, B.R. Stoner, L. Bergman, J.T. Glass and R.J. Nemanich, J. Appl. Phys. 69 (1991) 6400.
[5] K.F. Turner, Y.M. LeGrice, B.R. Stoner, J.T. Glass and R.J. Nemanich, J. Vac. Sci. Technol. B 9 (1991) 914.
[6] T.P. Humphreys, J.V. LaBrasca, R.J. Nemanich, K. Das and J.B. Posthill, Jpn. J. Appl. Phys. II 30 (1991) 1409.
[7] T. Tsuno, T. Imai, Y. Nishibayashi, N. Fujimori and K. Hamada, Jpn. J. Appl. Phys. I 30 (1991) 1063.
[8] M.P. Everson and M.A. Tamor, J. Vac. Sci. Technol. B 9 (1991) 1570.
[9] H.G. Busmann, H. Sprang, I.V. Hetel, W. Zimmermann-Edling and H.J. Guentherodt, Appl. Phys. Lett. 59 (1991) 295.
[10] J.A. Martin, L. Vazquez, P. Bernard, F. Comin and S. Ferrer, Appl. Phys. Lett 57 (1990) 1742.
[11] C.B. Collins, F. Devanloo, D.R. Jander, T.J. Lee, H. Park and J.H. You, J. Appl. Phys. 69 (1991) 7862.
[12] S. Ferrer, F. Comin, J.A. Martin, L. Vazquez and P. Bernard, Surf. Sci. 251/252 (1991) 960.
[13] C.B. Collins, F. Davanloo, E.M. Juengerman, D.R. Jander and T.J. Lee, Surf. Coat. Technol. 47 (1991) 754.
[14] N.H. Cho, D.K. Veirs, J.W. Ager III, M.D. Rubin, C.B. Hopper and D.B. Bogy, J. Appl. Phys 71 (1992) 2243.
[15] A.T. Collins, M. Kamo and Y. Sato, J. Mater. Res. 5 (1990) 2507.
[16] J.A. Freitas Jr., J.E. Butler and U. Strom, J. Mater. Res. 5 (1990) 2503.
[17] G.S. Gildenblat, S.A. Grot, C.W. Hatfield, A.R. Badzian and T. Badzian, IEEE Electron Devices Lett. 11 (1990) 371.
[18] K.L. Moazed, R. Nguyen and J.R. Zeidler, IEEE Electron Device Lett. 9 (1988) 350.
[19] H. Shiomi, H. Nakahata, T. Imai, Y. Nishibayashi and N. Fujimori, Appl. Phys. I 28 (1989) 758.
[20] J.W. Glesener and A.A. Morrish, K.A. Snail, J. Appl. Phys. 70 (1991) 5144.
[21] K.L. Moazed, J.R. Zeidler and M.J. Taylor, J. Appl. Phys. 68 (1990) 2246.
[22] M.C. Hicks, C.R. Wronski, G.S. Gildenblat, A.R. Badzian, T. Badzian and R. Messier, J. Appl. Phys. 65 (1989) 2139.
[23] F.J. Himpsel, P. Heimann and D.E. Eastman, Solid State Commun. 36 (1980) 631.
[24] J. van der Weide and R.J. Nemanich, in: Proceedings of the First International Conference on the Applications of Diamond Films and Related Materials, eds. Y. Tzeng, M. Yoshikawa, M. Murakawa and A. Feldman (Elsevier, New York, 1991) p. 359.
[25] T. Tachibana, B.E. Williams and J.T. Glass, Phys. Rev. B 45 (1992) 11975.
[26] B.B. Pate, M.H. Hecht, C. Binns, I. Lindau and W.E. Spicer, J. Vac. Sci. Technol. 21 (1982) 364.
[27] E.H. Rhoderick and R.H. Williams, Metal–Semiconductor Contacts (Clarendon Press, Oxford, 1988).